Proceedings of the 6th Nordic Signal Processing Symposium - NORSIG 2004
June 9 - 11, 2004
Espoo, Finland

Compression Gains in 2D MRCP Biliary Tree Modeling

Rajasvaran Logeswaran

Multimedia University
Faculty of Engineering, 63100 Cyberjaya
MALAYSIA
Tel. +603-8312 5419, Fax: +603-8318 3029
E-mail: loges@ieee.org

ABSTRACT

MRCP images are used to analyze the biliary tract in the diagnosis of liver diseases. As with many medical imaging techniques, MRCP are taken as a large series of images, usually including an amount of surrounding tissue, organs and acquisition noise. To minimize the storage requirements of patient medical history archives, and provide some assistance in reducing the influence of distracting noise in MRCP images diagnosis, the ROI may be modeled. Compression is derived from the lesser size of the models, thus saving on limited storage resources. This paper presents the compression gains through a technique for modeling of the hierarchical biliary tree structure in 2D MRCP images.

1. INTRODUCTION

Many modalities of medical imaging capture a series of images for location and orientation of the region of interest (ROI), slice images for 2D representation of 3D volume, images with different settings, sequences or parameters, and taken large enough to cover surrounding regions. These images are used for diagnosis and then stored as part of the patient medical history, taking up a lot of valuable storage space, especially when thousands of patient records have to be maintained over many years.

MRCP (Magnetic Resonance Cholangio Pancreatography) [1]-[2] is popular for diagnosis of pancreaticobiliary diseases due to its many favourable characteristics, including being non-invasive, non-ionising, flexible, non-hospitalization, fair image quality and inter-radiologist agreement, reduced dependence on operator and contrast medium. However, radiographers routinely capture a large number of images for a number of sequences (e.g. T1- and T2-weighted, thick and thin slices, orientation slices, projected 2D slices etc.) to ensure enough data and avoid subjecting patients to re-examination. Although such amounts of data may aid in the diagnosis stage, they are storage and processing intensive. After diagnosis, some storage could be recovered by storing only pertinent information through sub-sampling and reducing image background.

This paper proposes a technique of identifying the biliary tree characteristics for visual representation, evaluation and manipulation. The emphasis is on the compression gains derived from the proposed schemes, for image archiving after diagnosis. The schemes may be applied a-priori to conventional archiving compression techniques, e.g. arithmetic coding [3], Lempel-Ziv [3], JPEG 2000 [4], BZIP2 [5], ARJ [3] etc. The schemes should be easily adapted to the PACS (Picture Archiving Communication System) [6] and THIS (Total Hospital Information System) [7], even though they tend to be established on proprietary equipment and customizations, as the results cater for the common medical images storage in the DICOM (Digital Imaging and Communications in Medicine) [8] standard that contains dynamic header information and raw data, enabling retrieval of the data on the actual acquisition environment.

2. ALGORITHM

2.1 Pre-processing

Due to the acquisition technology, MRCP images usually suffer from noise, artefacts, volume effect, objects and organs overlapping or in very close proximity, bright spots, inconsistent image intensities, excessive image border and surrounding tissue etc. Pre-processing is vital for efficiency and reducing the disparity between images.

ROI Selection removes undesired regions, reduces the total image noise as well storage requirements, reduces image complexity and promotes increased processing speed. Labeling is required to identify structures that belong to the biliary tract, and may be done manually or semi-automated using algorithms such as PDM (Point Distribution Model) [9], splines [10] and snakes [11].

Image Normalization by first trimming the frequency histogram of the top and bottom 5% of intensities (experimentally, these were found to not contain significant information on the biliary tree), and scaling the intensities, reduces inherent MRCP image intensity variations, background noise and bright spots. As conventional systems display only 8 bits per pixel (bpp) intensities, rather than the 12 bpp raw image data in MRCP DICOM files, scaling the histogram for general purpose visualizers is also useful for remote access in telemedicine and web-based applications, and provides visual enhancement when image intensities are too low (structures unobservable) or too high (confusing representation as 12 bpp intensities are replaced by cycles of intensities 0-255, e.g. greyvalue 256 is represented as 0). Generally, it is the relative (c.f. actual) intensities that are used by medical practitioners, by frequently manipulating image contrast and brightness.

2.2 Multi-resolution Analysis

Multi-resolution analysis [12] is biologically motivated based on the visual process of realizing details incrementally (at different resolutions). Implementation is via low-pass filtering the image, with different values of the blurring coefficient σ and incrementing σ exponentially to provide good sampling even with a small set of σ. The Gaussian derivatives acts as an effective filter [13], possessing the qualities of: causality (reduces details, but does not introduce new features into the image), isotropy, scale invariance, location invariance, its partial derivatives are a solution for the diffusion equation, and has good performance [13].

Pixel-level operations are too susceptible to local minima, thus images are processed in clusters (segments) of pixels with similar characteristics. The watershed algorithm [14], applied on the image intensity, is used to identify segment boundaries (corresponds to branches). Each resolution is segmented separately. Very fine segments of similar characteristics may be merged to minimize local minima, but without losing too much fine resolution information for reproducing a detailed model.

In order to track a characteristic (e.g. biliary tree branch), segments from the highest resolution need to be mapped to each successive lower resolutions, through comparisons of the greatest overlap between segments in the corresponding layers. The segment shapes, sizes and numbers may vary slightly during merging. The lowest resolution at which each segment persisted is recorded.

2.3 Biliary Tree Representation

Using the analysis above, the hierarchical structure of the biliary tree is approximated through the segment persistence information. Three schemes have been implemented to represent this hierarchy information.

2.3.1 Hierarchical Plot

The higher intensity segment boundaries or ridges correspond to the location of branches of the biliary tree. Lower intensity segments usually represent background and may be removed. The ridges of interest are thinned to one pixel thickness using the hit-or-miss algorithm [15]. Nodes are identified as the meeting point of three or more ridges while sub-branches are identified as the ridge between two nodes. Using the information collected in the multi-resolution analysis, ridges are plotted, from those at the lowest resolution to the highest desired level, using varying plot thickness and appropriate color table to approximate the hierarchical biliary tree structure. The hierarchical information is stored in a matrix, as in (1).

$$ridges\_list = \begin{bmatrix} l_1 & x_{1,1} & y_{1,1} & x_{1,2} & y_{1,2} \\ l_2 & x_{2,1} & y_{2,1} & x_{2,2} & y_{2,2} \\ \vdots & \vdots & \vdots & \vdots & \vdots \\ l_m & x_{m,1} & y_{m,1} & x_{m,2} & y_{m,2} \end{bmatrix} \tag{1}$$

where l_m is the level (lowest resolution) ridge m persisted, and $((x_{m,1},y_{m,1}), (x_{m,2},y_{m,2}))$ = (start, end) coordinates of m.

2.3.2 Hierarchical Growing

The hierarchy plot gives a representation of the tree skeleton. A better representation of the tree branch orientation and thickness is by highlighting the corresponding segments rather than just the boundaries. For this scheme, additional segment information is required. In order to minimize the size of the model, it is sufficient to store the segmented image with each pixel intensity set to the highest level of its segment. To use the DICOM format, the model represented by (2) can be used to replace the raw data of the original file and adjusting the header information accordingly.

$$model = \begin{bmatrix} l_{1,1} & \cdots & l_{1,n} \\ \vdots & \ddots & \vdots \\ l_{m,1} & \cdots & l_{m,n} \end{bmatrix} \tag{2}$$

where $l_{m,n}$ = segment level (hierarchy) of pixel (m,n).

2.3.3 Segment Growing

Hierarchy growing uses segment boundaries as a guide for branch locations. Alternatively, region growing on the segments enables more control on determining if a segment is part of the tree. This scheme requires that the watershed segmentation be undertaken on the absolute gradient image rather than on the intensity image, so that the actual segment (c.f. segment boundary) is identified as a sub-branch. To minimize intensity inconsistencies, averaged segment intensities are used. The choice of seed segments to start the growing is based on several characteristics, such as intensity, segment size, connectedness and distance (the biliary tree is the focus of the ROI, so main branches are expected to be located close to the centre of the image), satisfying (3) and (4).

$$seed\_segment = \forall_{segments} . \exists_{segment} . \max(criteria_{segment}) \tag{3}$$

$$criteria = \mathrm{P}(intensity).intensity + \mathrm{P}(size).size + \mathrm{P}(distance).|distance| + \mathrm{P}(connectivity).connectivity \tag{4}$$

where $\mathrm{P}(x)$ is the significance of parameter x.

Table 1. Results, in terms of image size and compression ratio (CR), of the Border-trimmed and ROI selected images, and those achieved by the proposed Hierarchy Plot, Hierarchy Growing and Segment Growing schemes

Test File	Border Trimmed			ROI Selected Image					ROI Image (bpp)		$N_{segments}$	N_{nodes}	N_{ridges}	Hierarchy Plot		Hier. & Seg. Grow	
	Image (pixels)	12 bpp Size	CR	Image (pixels) N_x x N_y	12 bpp Size	CR	8 bpp Size S_{ROI}	CR	S_x	S_y				Size (bits) M_{plot}	CR	Size (bits) M_{grow}	CR
F1	196 x 170	399840	1.97	184 x 120	264960	2.97	176640	4.45	8	7	207	397	1815	61710	12.74	88320	8.90
F2	158 x 126	238896	3.29	128 x 112	172032	4.57	114688	6.86	7	7	80	140	664	21248	37.01	57344	13.71
F3	176 x 208	439296	1.79	96 x 104	119808	6.56	79872	9.85	7	7	50	97	527	16864	46.63	39936	19.69
F4	182 x 146	318864	2.47	184 x 160	353280	2.23	235520	3.34	8	8	217	412	1780	64080	12.27	117760	6.68
F5	158 x 184	348864	2.25	72 x 112	96768	8.13	64512	12.19	7	7	77	143	598	19136	41.10	32256	24.38
F6	124 x 134	199392	3.94	80 x 88	84480	9.31	56320	13.96	7	7	60	107	497	15904	49.45	28160	27.93
F7	174 x 152	317376	2.48	160 x 96	184320	4.27	122880	6.40	8	7	61	111	846	28764	27.34	61440	12.80
F8	168 x 174	350784	2.24	120 x 120	172800	4.55	115200	6.83	7	7	93	170	833	26656	29.50	57600	13.65
F9	196 x 150	352800	2.23	112 x 88	118272	6.65	78848	9.97	7	7	70	127	815	26080	30.15	39424	19.95
F10	134 x 128	205824	3.82	64 x 88	67584	11.64	45056	17.45	6	7	30	55	393	11790	66.70	22528	34.91
F11	256 x 256	786432	1.00	216 x 128	331776	2.37	221184	3.56	8	7	74	138	1072	36448	21.58	110592	7.11
F12	212 x 198	503712	1.56	208 x 120	299520	2.63	199680	3.94	8	7	360	696	2728	92752	8.48	99840	7.88
F13	176 x 180	380160	2.07	128 x 88	135168	5.82	90112	8.73	7	7	66	117	737	23584	33.35	45056	17.45
F14	168 x 190	383040	2.05	136 x 112	182784	4.30	121856	6.45	8	7	99	179	1148	39032	20.15	60928	12.91
Avg	**177 x 171**	**373234**	***2.11***	**135 x 110**	**184539**	***4.26***	**123026**	***6.39***	***8***	***7***	**110**	**206**	**1032**	**61710**	***22.75***	**61513**	***12.78***

A number of seeds are needed as parts of the tree structure in the volume axis are disjoint in slice images. Segment growing guides include average segment intensity, intensity difference, direction of growth, connectivity, and segment size, with the rules customized experimentally and enhanced dynamically. As before, only the segmented image with the pixel intensity values representing the levels, are stored. This resulting model is compatible with the DICOM file format.

3. RESULTS

The results of applying the technique on a number of 2D MRCP images, acquired from the collaborating medical institution, are summarized in Table 1 and Fig. 1.

3.1 Compression in Pre-processing

Each original image (Fig. 1(a.1)) is 256 x 256 pixels, 12 bpp, totalling 786432 bits, and with varying amounts of image border (no border in F11 and up to almost half of the 3D projected image F6). Border trimming itself provides reasonable compression (Table 1). For ROI selection with the 12 bpp and 8 bpp representations given in the table, compression performance of the 8 bpp representation shows compression of up to 17 times is achievable through just the pre-processing stage alone.

3.2 Compression in Modeling

The results achieved by the proposed schemes are given in the shaded part of Table 1, along with the total number of segments ($N_{segments}$), nodes (N_{nodes}) and ridges (N_{ridges}) identified at the highest resolution. The biliary tree model sizes are calculated with (4) and (5).

$$M_{plot} = N_{ridges} (S_{level} + 2 (S_x + S_y)) \quad (4)$$

$$M_{grow} = N_x \, . \, N_y \, . \, S_{level} \quad (5)$$

where M_{plot} = size of the hierarchy plot scheme model, M_{grow} = size of the model for the hierarchy grow and segment grow schemes, (N_x x N_y) = image dimensions (pixels) of the ROI selected image, and (S_x x S_y) = number of bits to represent the ROI selected image. S_{level} = size (in bits) used to represent the number of levels. S_{level} is assumed to be 4 bits but larger word sizes may be used if finer levels are required. Segmentation that is too fine may not be well visualized and is not efficient as it more processing intensive. Levels can be grouped.

From Table 1, it is found that the hierarchical plotting scheme was successful in achieving the best compression (average CR of 22.75, maximum CR above 60). However, the hierarchical plot (Fig. 1(d.3)) is too lossy to reproduce a good representation of the biliary tree, but may have applications as an overlay on other techniques to examine the intricacies in some MRCP images, and with it's small size, may be stored easily for supplementary use. The hierarchical growing (Fig. 1(e.3)) and segment growing (Fig. 1(f.3)) schemes produced the same results (average CR of 12.78, and up to 34.91), due to the similar data storage strategy. From a quality point of view, segment growing is preferred as it gives better control in identifying the tree. The merits of both could be integrated to produce an improved scheme.

4. CONCLUSION

The three schemes proposed managed to achieve substantial compression performance. Of these, the more practical scheme, segment growing, was successful in achieving an average CR of 12.78 on 2D MRCP images, with compression performance exceeding 20 times for some test files. The benefit of this scheme is that the model, in the form of a segmented image with the pixel intensity values set to the hierarchical level of the biliary tree structure, can be easily stored in the common DICOM medical image standard. For archiving, any

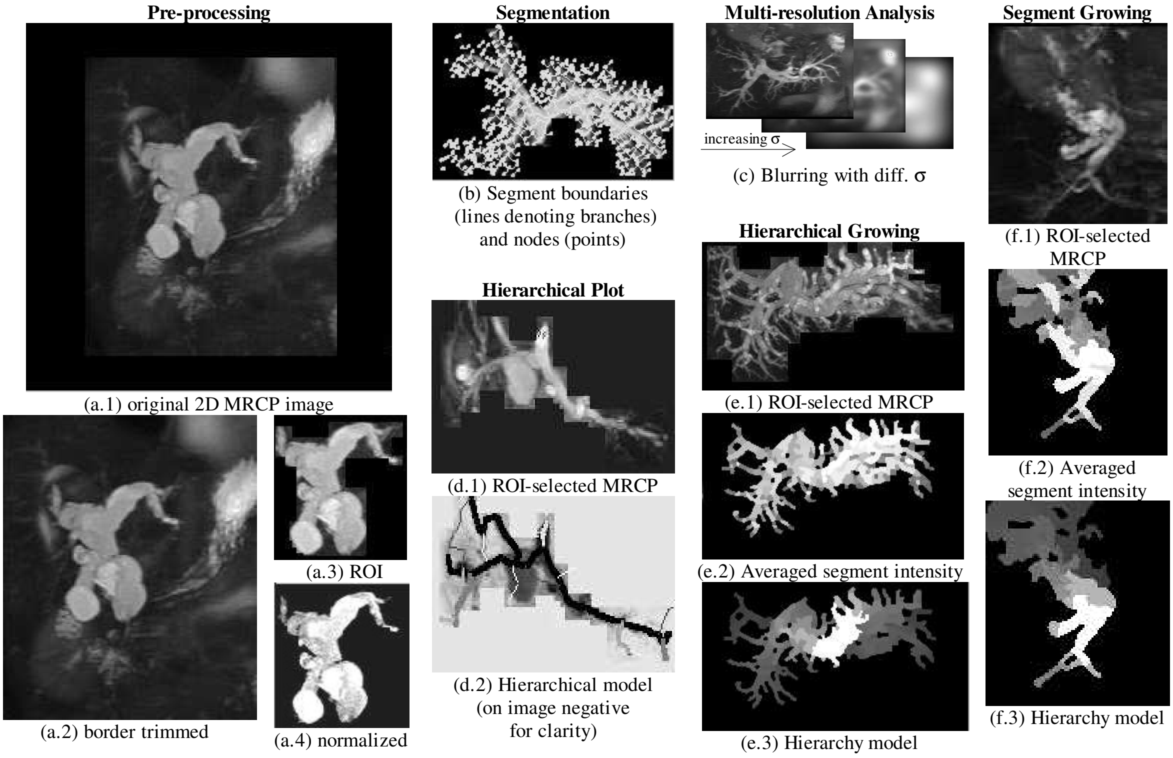

Fig. 1. MRCP images showing the results of pre-processing, segmentation and modeling with the proposed schemes

default or proprietary compression algorithms used on the DICOM files could be used on this scheme. Even simple run-length coding [3] would work better on the model than on the original image as similar intensities are clustered. For diagnosis accuracy and legal considerations, the proposed scheme is recommended for use after diagnosis, in long-term archiving of patient medical records. Furthermore, with the flexibility of the scheme, certain pertinent MRCP images may be stored in their original form, whereas routine images could be modeled. As the same file format can be used, visualization and manipulation of the model could be conducted in a similar fashion as the original images, and on the same hardware and software combinations. Potential improvements include the use of adaptive algorithms, better knowledge collection and analysis, added 3D visualization and inter-slice modeling.

ACKNOWLEDGEMENT

This work has benefited from contributions by Selayang Hospital (Malaysia), Michel Bister (University of Nottingham, Malaysia) and Pechin Lo (Multimedia University, Malaysia).

REFERENCES

[1] Justus, S. Govil and I. Korah, “Non-Breath-Hold Magnetic Resonance Cholangiography – Preliminary Results and Review of Literature”, *Indian J. of Radiology and Imaging*, vol. 9, no. 2, 1999, pp. 53-58.

[2] Y. Yamashita, Y. Abe, Tang, Urata, S. Sumi and M. Takahashi, “In Vitro and Clinical Studies of Image Acquisition in Breath-Hold MR Cholangiopancreatography: Single-Shot Projection Technique versus Multislice Technique”, *AJR*, vol. 168, 1997, pp. 1449-1454.

[3] M. Nelson and J.-l. Gailly, *The Data Compression Book, 2nd ed.*, NY, USA: M&T Books, 1995.

[4] D.S. Taubman and M.W. Marcellin, *JPEG 2000: Image Compression Fundamentals, Standards and Practice*, Kluwer Int. Series in Engineering and Computer Sci., Secs 642, 2001.

[5] J. Seward, *The bzip2 and libbzip2 official home page*, 2002, http://sources.redhat.com/bzip2/.

[6] H.K. Huang and R.K. Taira, “Infrastructure design of a picture archiving and communication system”, *American J. of Roentgenology*, vol. 158, 1992, pp. 743-749.

[7] Y. Kurihara, Y. Okuhara, Y. Narita, Y. Kitazoe, A. Sawada and S. Yoshida, “Integration of Medical Images into the Total Hospital Information System - Experiences at Kochi Medical School”, *32nd Annual Hawaii Int. Conf. on System Sci.* vol. 4, 1999, pp. 1-8.

[8] ACR/NEMA, *Standards Publication PS3 / DICOM 3 (Digital Imaging and Communications in Medicine Standard)*, 1993.

[9] T.F. Cootes, A. Hill, C.J. Taylor and J. Haslam, “The Use of Active Shape Models For Locating Structures in Medical Imaging”, *Proc. IPMI'93*, Flagstaff, USA, 1993, pp. 33-47.

[10] Bartels, Beatty, and Barsky, *An Intro. to Splines for Use in Comp. Graphics and Geometric Modeling*, Morgan Kaufmann, 1987.

[11] L.-Y. Yu and C. Dyer, "Perception-based 2d shape modelling by curve shaping", *4th Int. Workshop on Visual Form, Lecture Notes in Computer Sci.*, Springer-Verlag, 2001.

[12] L. Florack, B. Romeny, J. Koenderink and M. Viergever, “Scale and the differential structure of images”, *IVC*, vol. 10, 1992, pp. 376–388.

[13] B. Romeny, *Front-end Vision and Multi-scale Image Analysis*, Holland: Kluwer, 2002.

[14] S. Beucher, and C. Lantuejoul, “Use of Watersheds In Contour Detection”, *Int. Workshop on Image Processing, Real-time Edge and Motion Detection/Estimation*, Rennes, France, 1979.

[15] R.C. Gonzalez and R.E. Woods, *Digital Image Processing, 2nd ed.*, NJ, USA: Prentice Hall, 2002.